Check for updates

Study of magnetocaloric properties of small Bi-doped $Pr_{0.55}Ca_{0.05}Ba_{0.40}Mn_{1-x}Bi_xO_3$ manganites

Gönül Akça[1,*] , Selda Kılıç Çetin[1], and Ahmet Ekicibil[1]

[1] *Department of Physics, Faculty of Sciences and Letters, Çukurova University, 01330 Adana, Turkey*

ABSTRACT

Here, we investigated the magnetic and magnetocaloric (MC) properties of manganites labeled PrCaBaMnO and PrCaBaMnBiO, with compositions $Pr_{0.55}Ca_{0.05}Ba_{0.40}Mn_{1-x}Bi_xO_3$ (x = 0 and 0.02), respectively. The solid-state reaction method was used for sample preparation, and the structural properties were checked using X-ray diffraction (XRD). Temperature dependence of magnetization ($M(T)$) measurements was carried out in the range of 5–300 K under 100 Oe field to determine the transition temperature of the manganites. Magnetic entropy change ($-\Delta S_M$) values were computed from field-dependent magnetization ($M(H)$) measurements. For the 2 T magnetic field values, the $-\Delta S_M^{max}$ values for the PrCaBaMnO and PrCaBaMnBiO manganites are 3.15 and 2.86 Jkg^{-1}K^{-1}, respectively. Relative Cooling Power (RCP) values were calculated from the temperature dependence of $-\Delta S_M$ (T) curves, resulting in 82.4 and 88.6 Jkg^{-1} for PrCaBaMnO and PrCaBaMnBiO, respectively. Banerjee's criterion and Franco's universal master curve confirmed that the transition type for the studied manganites is second order.

1 Introduction

Refrigeration and air conditioning technologies, commonly referred to as traditional cooling systems, play a vital role in our daily lives, relying on the compression/expansion principle of gases. These systems, which remain at low levels compared to other systems in terms of energy efficiency, have high energy consumption. In these systems, which are known to reach thermodynamically limited values, high-vibration compressors are used that cause high energy consumption and excessive noise. Additionally, gases used in these systems as refrigerants have adverse effects on the environment [1]. Consequently, there is a need for research and regulations to reduce the energy consumption in refrigeration and air conditioning processes and reduce the effects of traditional systems on the environment.

Refrigeration systems based on different thermodynamic effects have been developed to replace these conventional systems [2]. Among these alternatives, magnetic refrigeration (MR) systems are more advantageous in terms of energy consumption and efficiency and are considered the future of the cooling technologies [3]. MR systems operate based on the magnetocaloric effect (MCE) principle, which is

Address correspondence to E-mail: gdayan@cu.edu.tr

Springer

one of the reversible thermodynamic effects with potential applications in various technologies [4–6]. MCE is the observed change in temperature of the material due to the change in entropy of the magnetic material as a result of exposure to an external magnetic field. This effect involves two fundamental processes: adiabatic temperature change (ΔT_{ad}) and magnetic entropy change ($-\Delta S_M$) [7]. The most essential condition for designing a magnetic cooler is to obtain magnetic material with a high $-\Delta S_M$ and a high ΔT_{ad} value within the operating temperature range [8]. MR systems have been developed in which Gd and Gd-based alloys are used as cooling substances [9]. The practical application of these material systems has not been feasible for some critical reasons [5]. Factors affecting their commercial use include high raw material costs, challenging and complex production techniques, high thermal and magnetic hysteresis, etc. [10] Materials that can be used as cooling materials should not have these and similar negative features. Considering these criteria, manganites are among the material groups with high potential to be considered as a suitable cooling element for MR systems. Although the manganites have relatively low $-\Delta S_M$ values compared to other material groups, they have desirable properties such as low raw material cost, simple and inexpensive production techniques, and a second-order phase transition (SOMT). One of the reasons why manganites are in a more advantageous position compared to other material groups is that their magnetic phase transition temperature (T_C) can be adjusted with doping [10].

The structural properties of manganites have a great impact on their magnetic and MC properties. Therefore, it is necessary to briefly mention the structural properties of manganites. Manganites are a group of materials represented by the chemical equation with ABO_3, crystallizing in the perovskite structure, and containing manganese ions as the B-site element [11]. Numerous investigations have been conducted to examine the magnetic and MC properties of La and Pr-based manganites [11–15]. In many of these studies, it is aimed to investigate the effects of factors such as change in the average ionic radius of the A-site , Mn^{3+}/Mn^{4+} ratio, cationic mismatch effect, sintering temperature, and doping of A and B-sites [14, 16–20]. The structural, magnetic, and MC properties of $Pr_{0.55}Ca_{0.05}Ba_{0.40}Mn_{1-x}Bi_xO_3$ ($x = 0$ and 0.02) manganites, which have not been studied before, are presented

in this study. The results of the analysis and measurements performed to examine the structural, magnetic, and MC properties of the samples are given in detail.

2 Experimental procedure

In this study, the solid-state reaction method was chosen due to its simplicity and ease of application for sample preparation. Detailed information about the processes of the method has been provided in our previous work [11, 20]. Sigma Aldrich brand Pr_2O_3 (99.9%), CaO (99.995%), BaO (99.995%), Bi_2O_3 (99.99%), and MnO_2 (99.99%) chemicals were used in sample production. Stoichiometric amounts of these starting chemicals were ground and mixed in an agate mortar for 6×10 minutes. The powder mixture was calcined in air at 600 °C for 6 hours. After this process, a second grinding process was applied under the same conditions (for 6×10 minutes for a total of 60 minutes). Then, the powder sample was pressed to form tablets. The tablets were subjected to the sintering process at 1200 °C for 24 hours. The synthesized samples $Pr_{0.55}Ca_{0.05}Ba_{0.4}Mn_{1-x}Bi_xO_3$ ($x = 0$ and 0.02) have been labeled as PrCaBaMnO for $x = 0$ and PrCaBaMnBiO for $x = 0.02$, respectively. To determine the crystal symmetry and phase purity of the samples, X-ray diffraction (XRD) measurements were executed at room temperature. The surface morphology of the PrCaBaMnO and PrCaBaMnBiO manganites was analyzed using scanning electron microscopy (SEM). The magnetic measurements were performed by a physical property measurement system (PPMS) equipped with a vibrating sample magnetometer (VSM) module.

3 Results and discussions

The diffraction patterns obtained from XRD analyses of PrCaBaMnO and PrCaBaMnBiO manganites are presented in Fig. 1. In the diffraction patterns of the manganites, the red dots and solid black lines represent observed and calculated data, respectively. The green ticks show Bragg diffraction positions. The difference between the calculated and observed data is illustrated by the blue line. Sharp and narrow-based diffraction peaks interpreted as good and homogeneous crystallization of the samples are seen from the XRD patterns [21]. A very weak diffraction peak consistent with the $BaMnO_{2.98}$ impurity phase was
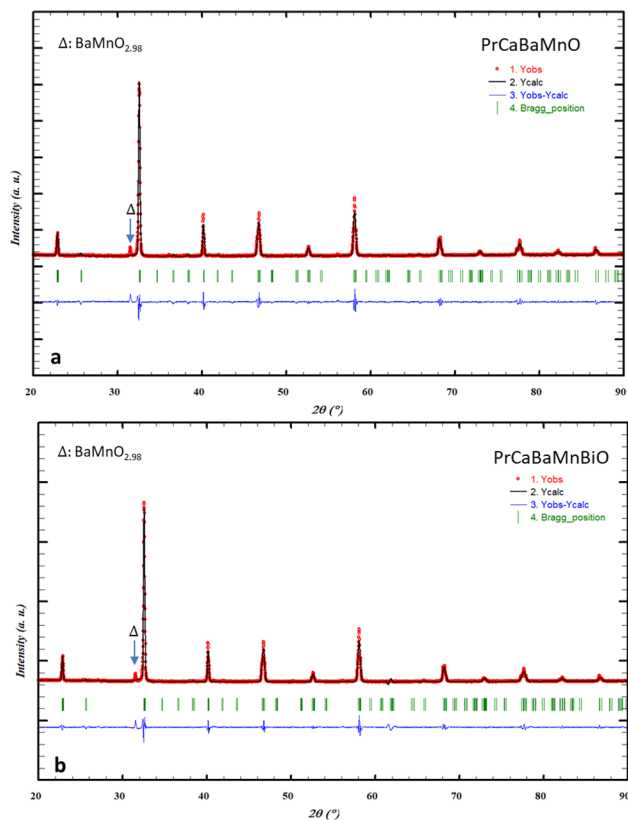
Fig. 1 XRD patterns of the studied manganites

Table 1 The lattice parameters and the V values of PrCaBaMnO and PrCaBaMnBiO manganites

Sample codes	PrCaBaMnO	PrCaBaMnBiO
a (Å)	5.492 (7)	5.494 (1)
b (Å)	5.501 (3)	5.491 (2)
c (Å)	7.816 (8)	7.798 (1)
V (Å³)	236.200 (1)	235.262 (4)
χ^2	4.33	4.85
R_p	3.75	3.57
R_{wp}	5.63	6.06
R_{exp}	2.71	2.75
t	0.938	0.935
β (°)	0.1863	0.180
D_{XRD} (nm)	44.51	46.00

distortion and hybridize with oxygen's 2p orbitals [16]. The change in lattice parameters and decrease in V value may affect the magnetic and MC properties. The stability of the perovskite structure is controlled by the Goldschmidt tolerance factor (t_G) given below [26]:

$$t_G = \frac{(\langle r_A \rangle + r_O)}{\sqrt{2}(\langle r_B \rangle + r_O)}. \tag{1}$$

The terms of $\langle r_A \rangle$ and $\langle r_B \rangle$ given in the equation state the mean ionic radii of A and B-sites, respectively. The term r_O is the ionic radius of the oxygen ion. For PrCaBaMnO and PrCaBaMnBiO manganites, the t_G values have been calculated based on Shannon's effective ionic radii list [24]. The t_G values of the studied manganites are represented in Table 1. The obtained values confirm that the samples crystallize in the perovskite structure [27, 28]. The t_G values calculated for the samples are compatible with the orthorhombic structure. As expected, a decrease in t_G has been observed with doping Bi at a concentration of $x = 0.02$ to the Mn-site since Bi^{3+} ions have larger ionic radii than Mn^{3+} ions [24]. The average crystalline size (D_{XRD}) of the PrCaBaMnO and PrCaBaMnBiO manganites was calculated using the Debye Scherrer equation as follows [20].

$$D_{XRD} = \frac{\kappa \lambda}{\beta \cos \theta}, \tag{2}$$

where λ is the x-ray wavelength (λ=1.54060 Å), κ is the grain shape factor, β denotes the full width at half maximum of the most intense peak, and θ is the Bragg

detected in the diffraction patterns of both samples, showing antiferromagnetic (AFM) properties [22]. The volume fraction of the impurity phase [23] is 3.6 % and 3.5 % for PrCaBaMnO and PrCaBaMnBiO manganites, respectively. The diffraction peaks of the studied manganites overlap with the *Pbnm* space group belonging to the orthorhombic crystal structure. In Table 1, lattice parameters and unit cell volume (V) acquired from the XRD refinement for PrCaBaMnO and PrCaBaMnBiO manganites using FULLPROF software are provided. Although a change in the lattice parameters was detected with the addition of Bi, no change in the crystal structure was observed. As seen from Table 1, the unit cell volume (V) of the PrCaBaMnBiO manganite is smaller than that of PrCaBaMnO manganite. Although an increase in the V value was thought due to the larger ionic radius of the Bi ion, a decrease in V value was noticed [24]. It is thought that this decrease is a result of the chemical pressure induced in the Mn octahedral as a consequence of the change in lattice parameters [25]. This decrease may also be attributed to the electronic configuration of Bi^{3+} ions that are identified by their $6s^2$ electrons which can create local

diffraction angle. In Table 1, the calculated β and D_{XRD} values are provided. It is released that the β value decreases with the Bi substitution for Mn, leading to an increase in the D_{XRD} value. The discrepancy in the ionic radii of the Mn^{3+} and Bi^{3+} ions may contribute to an enhancement in D_{XRD} values.

To investigate surface morphology and determine the average particle size (D) of the manganites, SEM images at 20 kx magnification were attained (inset of Fig. 2). The SEM images of both samples show particles of different sizes and shapes and intergranular spaces. Grain boundaries are more apparent for PrCaBaMnBiO manganite than that of the other. Therefore, we can say that the sharpness of the grain boundaries increases with the Bi substitution. ImageJ software was used to determine the D of the manganites. The size of 100 randomly selected particles was measured with this program and their histograms were obtained (See Fig. 2). The histograms reveal granular structures of different sizes in both samples. The average particle size (D_{SEM}) was approximately determined by Gaussian fit. D_{SEM} for the PrCaBaMnO and PrCaBaMnBiO manganites was determined as 0.79 and 0.83 μm, respectively. Although the particle size and the clarity of the grain boundaries are positively influenced by the Bi substitution, an increase in the volume of the intergranular spaces is also observed. The magnetic and MC properties of the studied manganites may decrease due to the deterioration of intergranular conduction with the increased volume of intergranular spaces. When compared to the D calculated from SEM

and XRD, it is observed that the D_{SEM} is higher than that of D_{XRD}. It implies that the grains are formed by several crystallites due to internal stresses or defects in the structure. The agglomeration degree, indicating the average number of crystallites forming a single grain, is determined by the D_{SEM}/D_{XRD} ratio [29].

To determine the T_C values of PrCaBaMnO and PrCaBaMnBiO manganites, low field $M(T)$ measurements were made in both the ZFC and FC processes under a magnetic field of 100 Oe and in the temperature range of 5–300 K. The $M(T)$ curves of PrCaBaMnO and PrCaBaMnBiO manganites are given in Fig. 3. When the $M(T)$ curves were examined, it is observed that the samples exhibit a particular magnetization value at low-temperature values, and the magnetization value decreases with increasing temperature and rapidly drops to zero. The temperature at which the magnetization value decreases to zero occurs represents the magnetic phase transition temperature, T_C. This change observed in the $M(T)$ curves is a transition specific to FM materials, and the material showed a transition to paramagnetic (PM) phase in T_C. The decrease in the magnetization value of the samples as the temperature increases is due to the increasing thermal interaction energy disrupting magnetic couplings in the structure [30]. Although the temperature-dependent variations of the curves obtained in the ZFC and FC processes behave similarly at temperatures above T_C, these curves in the low-temperature region exhibit different behaviors. The ZFC curves for both samples
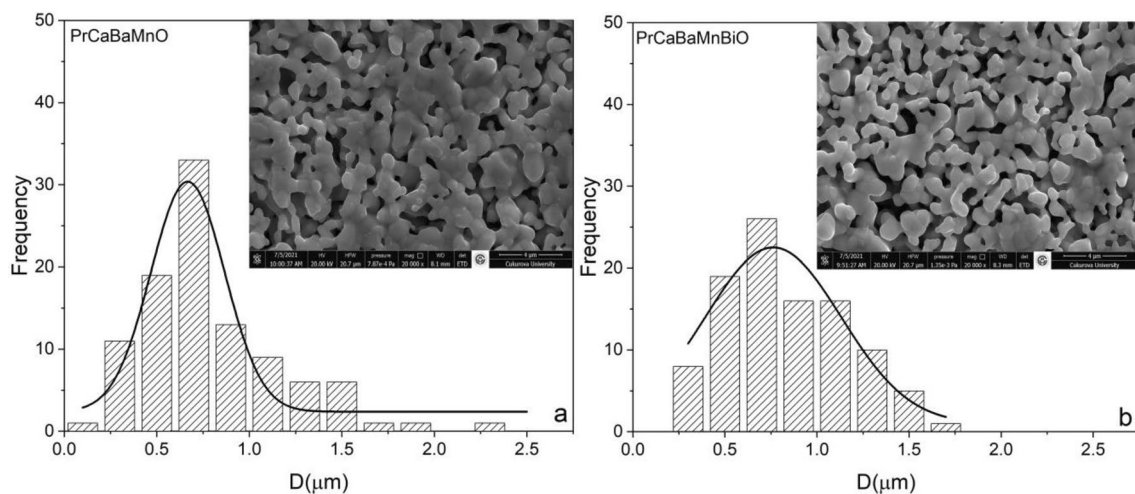
Fig. 2 The size distribution histograms of PrCaBaMnO (**a**) and PrCaBaMnBiO (**b**) manganites. The inset shows SEM images at 20 kx magnification for the studied manganites
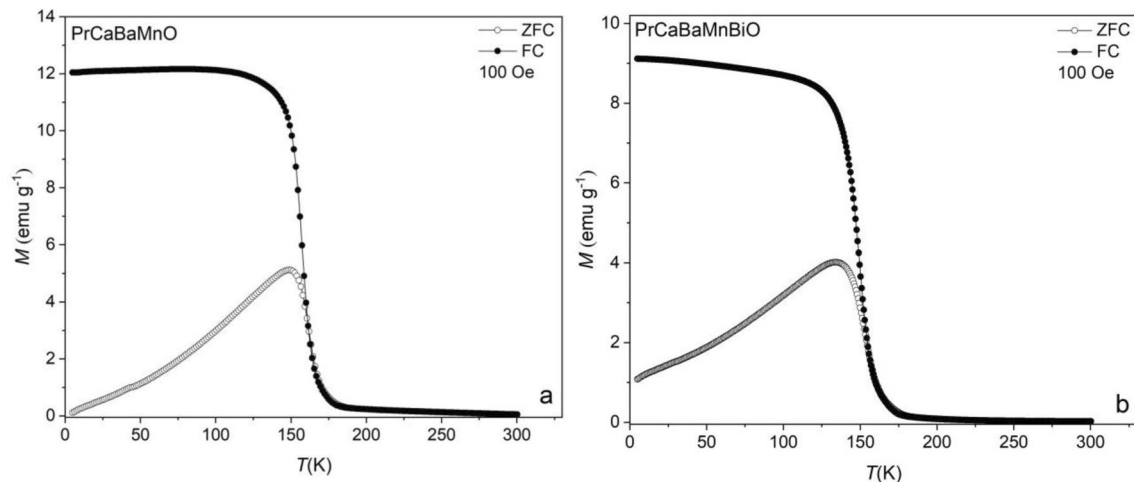
Fig. 3 The $M(T)$ curves which obtained at ZFC and FC modes under 100 Oe magnetic fields for PrCaBaMnO (**a**) and PrCaBaMnBiO (**b**) manganites

enhance with increasing temperature. This behavior may be due to the coexistence of AFM and FM clusters [31]. For both samples, a separation is observed in the low-temperature region due to the different temperature dependence of the ZFC and FC curves. The separation observed at low temperatures indicates that the samples exhibit a spin-glass-like behavior [32–34]. This separation allows us to have an idea about the long-range or short-range magnetic interaction in the material and the magnitude of the magnetic anisotropy of the structure [34, 35]. Materials with high magnetic anisotropy exhibit spins ordered in a preferential orientation, and in the ZFC process, their spins remain locked in random orientations. If a magnetic field is applied to the material after the cooling process, the measured magnetization value changes depending on the anisotropy of the material. Systems with high magnetic anisotropy may exhibit a low magnetization value in the ZFC curve at low temperatures, as the applied field strength may not be sufficient to direct the spins, resulting in differences between the magnetization curves measured during cooling in the FC process. When the magnetization value increases, the lower the magnetization value of the ZFC curve at low temperatures, the higher the anisotropy of the structure [36]. Considering the explanations given above, it can be said that the magnetic interaction is short-range [37]. The T_C values were determined by obtaining the dM/dT-T curve from the $M(T)$ data obtained in the ZFC process. This is one of the most widely used methods to

determine the T_C value. In this method, the temperature value corresponding to the minimum point of the dM/dT-T curve gives the T_C value. The T_C values of PrCaBaMnO and PrCaBaMnBiO manganites were determined as 164 and 154 K, respectively. The observed decrease in the T_C value with Bi substitution to the Mn-site may be due to the weakening of double exchange (DE) interactions [38, 39]. In addition, it is seen that the magnetic phase transition of the Bi-doped sample occurs in a wider temperature range than that of undoped manganite. A large value of $-\Delta S_M$ is generally observed when the magnetic phase transition occurs sharply [40] and the expansion in the magnetic phase transition temperature range with Bi-element substitution into the Mn-site can cause a decrease in the $-\Delta S_M$ value.

The $M(H)$ curves of PrCaBaMnO and PrCaBaMn-BiO manganites obtained from $M(H)$ measurements performed under 0–5 T field change at 4 K temperature intervals around T_C are given in Fig. 4. In the low-temperature region, it is observed that the magnetization values initially increase rapidly with the field and reach saturation above a field value of 0.5 T. No further change in magnetization value is observed with increasing field. This is characteristic of ferromagnetic materials and is the result of the orientation of all magnetic moments in the direction of the field. In the high-temperature region (above T_C), the $M(H)$ curves exhibit a linear variation with the applied field, representing paramagnetism. In summary, the transition from the FM state to the
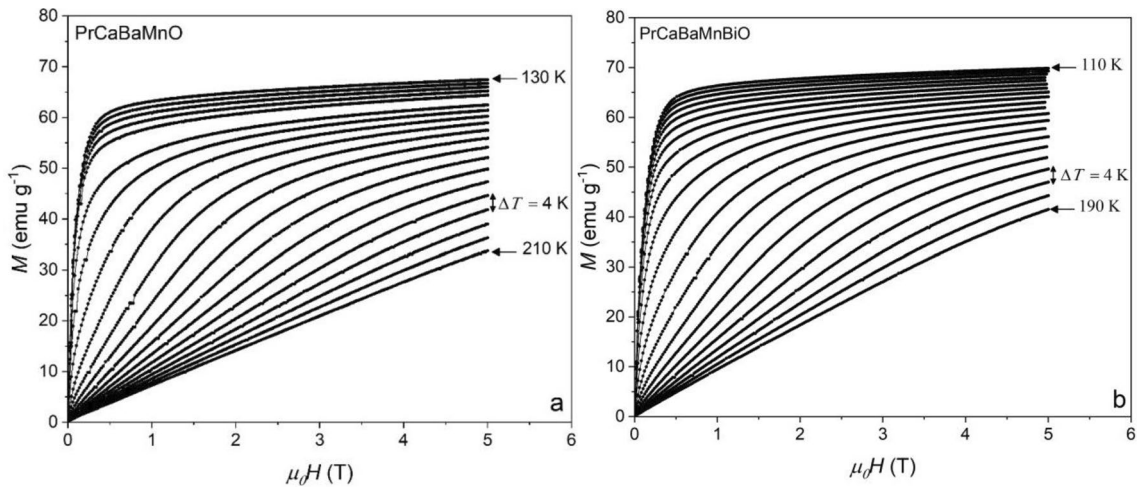
Fig. 4 The $M(H)$ curves for PrCaBaMnO (**a**) and PrCaBaMnBiO (**b**) manganites

PM state observed in the $M(T)$ measurements is also clearly seen in the $M(H)$ curves.

The main components defining the MCE are the $-\Delta S_M$ ve ΔT_{ad} values. Indirect measurement methods are commonly used to determine the $-\Delta S_M$ value. Initially, the T_C of the samples is identified, and isothermal $M(H)$ measurements are performed around the T_C. The numerical value of the $-\Delta S_M$ value can be determined by using the data obtained from these measurements and the following equation.

$$-\Delta S_M(H, T) = \sum \frac{M_i - M_{i+1}}{T_{i+1} - T_i} \Delta H_i \qquad (3)$$

The terms M_i and M_{i+1} given in Eq. (3) are abbreviations that express magnetization values at T_i and T_{i+1} temperatures, respectively. The $-\Delta S_M(T)$ curves obtained for various magnetic field change (ΔH) values of PrCaBaMnO and PrCaBaMnBiO manganites are given in Fig. 5. When the curves are examined, it is seen that it gives a maximum peak around T_C, which is called the maximum $-\Delta S_M(-\Delta S_M^{max})$ value [41]. It is observed that there is an enhancement in $-\Delta S_M^{max}$ values due to the increase in magnetization of PrCaBaMnO and PrCaBaMnBiO manganites with the increase of the external applied field. In addition, it is observed that the peak position of $-\Delta S_M^{max}$ for PrCaBaMnO and PrCaBaMnBiO manganites moves to
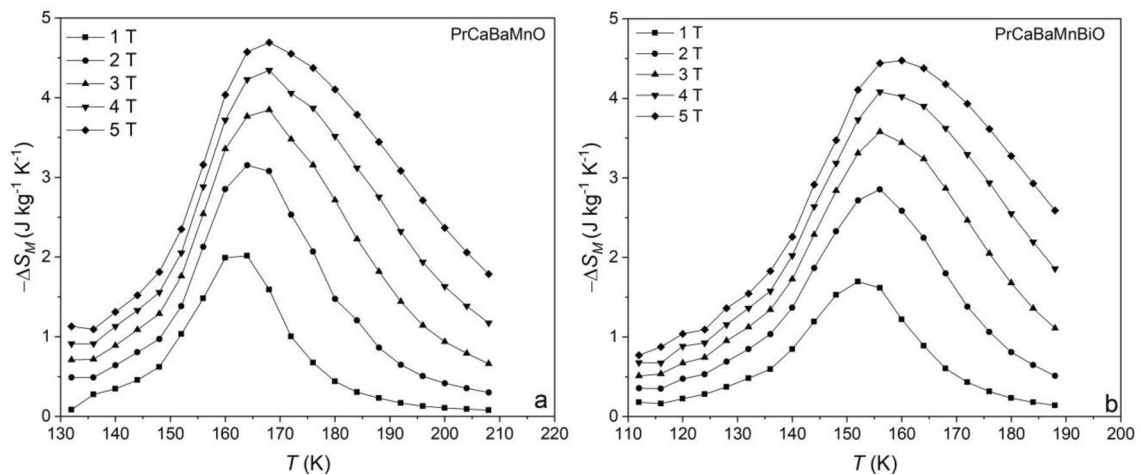

Fig. 5 The temperature dependence of the $-\Delta S_M$ curves under different magnetic fields for PrCaBaMnO (**a**) and PrCaBaMnBiO (**b**) manganites

high temperature with increasing magnetic field. This behavior may arise from the magnetic field dependence of the T_C [42, 43]. For the PrCaBaMnO manganite, the $-\Delta S_M^{max}$ value calculated under 2 T magnetic field was calculated as 3.15 $Jkg^{-1}K^{-1}$. Under the same magnetic field value, this value is 2.86 $Jkg^{-1}K^{-1}$ for the PrCaBaMnBiO manganite. According to the results obtained, the replacement of the Bi-element with Mn at low rates causes a decrease in the value of $-\Delta S_M^{max}$. It is considered that this decrease is due to the increase in the volume of intergranular spaces obtained from SEM analyses and the reduction in particle sizes.

For MS systems, the magnetic material must meet particular criteria to be considered a cooling element [44]. Although the material has high $-\Delta S_M$ ve ΔT_{ad} values under low field is the primary condition for being considered as a candidate cooler, it is not sufficient to meet this criterion. Apart from these two parameters, the RCP value, which determines the cooling capacity of the MS system to be designed, must be high and the hysteresis (thermal and magnetic) effect affecting the performance of the cooler must be negligible [11]. Thermal hysteresis is associated with the reversibility of the MCE of a magnetic heat sink, while magnetic hysteresis is connected to the operating efficiency of a magnetic heat sink [10]. The RCP value of the materials is calculated by $RCP = \left| -\Delta S_M^{max} \right| \times \delta T_{FWHM}$ equation. The δT_{FWHM} term is the full width at half the maximum of the $-\Delta S_M (T)$ curve. For PrCaBaMnO and PrCaBaMnBiO manganites, the RCP values were calculated as 82.4 and 88.6 Jkg^{-1} under 2 T magnetic fields, respectively.

Although the $-\Delta S_M^{max}$ value of PrCaBaMnBiO manganite is lower than PrCaBaMnO, its RCP value is higher. This result may stem from the magnetic phase transition occurring in a broader temperature range of the PrCaBaMnBiO manganite. In order to compare the results obtained with the literature, the $-\Delta S_M^{max}$ and RCP values of some Pr-based manganites for varied ΔH values are given in Table 2.

It is necessary to identify the type of magnetic phase transition of materials that can be used as cooling substances in MS systems. Materials in which the phase transition is attended by a structural transition exhibit First-Order Magnetic Transition (FOMT). The use of materials that exhibit transition of this type in technological applications is not suitable because the performance of the magnetic cooler is adversely affected. Second-order magnetic transition (SOMT) materials have high potential for applications. This transition of magnetic materials exhibiting SOMT usually occurs over a wide temperature range, and as a result, high RCP values may be achieved. There are many methods used to determine the type of magnetic phase transition [45–49]. The widely used method for determining the type of magnetic transition is the Banerjee criterion [45]. In this criterion, $H/M–M^2$ curves (described as Arrott plots) are obtained by using the data obtained from isothermal $M(H)$ measurements. Considering the sign of the slopes of these curves around T_C, the type of magnetic transition is decided. The positive slope of the Arrott curves around T_C implies that the type of magnetic transition is second order. The negative slope states that the kind of magnetic phase transition is first

Table 2 Summary of $-\Delta S_M^{max}$ and RCP values for some magnetocaloric samples at different magnetic fields

Sample	ΔH (T)	$-\Delta S_M^{max}$ ($Jkg^{-1}K^{-1}$)	RCP (Jkg^{-1})	Refs.
PrCaBaMnO	2	3.15	82.4	Present work
PrCaBaMnBiO	2	2.86	88.6	Present work
PrCaBaMnO	5	4.78	116.6	Present work
PrCaBaMnBiO	5	4.40	106.3	Present work
$Pr_{0.55}Na_{0.05}Sr_{0.4}MnO_3$	2	1.75	–	[52]
$Pr_{0.8}K_{0.2}MnO_3$	2	1.88	82.5	[53]
$Pr_{0.6}Sr_{0.4}MnO_3$	2	2.46	78.0	[54]
$Pr_{0.55}Sr_{0.45}MnO_3$	2	1.71	143.64	[55]
$Pr_{0.55}Sr_{0.35}K_{0.1}MnO_3$	2	2.20	86.0	[56]
$Pr_{0.7}Ca_{0.3}Mn_{0.8}Cr_{0.2}O_3$	2	1.5	–	[57]
$Pr_{0.7}Ba_{0.2}Ca_{0.1}MnO_3$	5	2.2	261	[58]
$Pr_{0.67}Ba_{0.63}MnO_3$	4	5.5	225	[59]
$Pr_{0.7}Ca_{0.3}Mn_{0.9}Ni_{0.1}O_3$	2	1.46	101.62	[60]

order. In light of these statements, the Arrott curves were obtained to determine the type of magnetic phase transitions of PrCaBaMnO and PrCaBaMnBiO manganites (Fig. 6). The Arrott curves of the PrCaBaMnO and PrCaBaMnBiO manganites have a positive slope around T_C. Consequently, it can be said that the magnetic phase transition of the studied manganites is of the second order. To check whether the methods used in determining the type of magnetic phase transition are compatible with each other, the phenomenological method proposed by Franco et al known as the universal master curve was also used [47, 50]. In this method, the rescaled temperature (θ) dependence of $-\Delta S_M(T)/-\Delta S_M^{max}$ is obtained. The θ is calculated from the following equations;

$$\theta = \begin{cases} -(T - T_C)/(T_{r1} - T_C) & T \le T_C \\ (T - T_C)/(T_{r2} - T_C) & T > T_C \end{cases}, \tag{5}$$

where T_{r1} and T_{r2} are the temperatures above and below T_C, respectively. In this approach, if the curves obtained for different ΔH values collapse to a single curve, the nature of magnetic phase transition is second order [51]. The $-\Delta S_M(T)/-\Delta S_M^{max}(\theta)$ curves for PrCaBaMnO and PrCaBaMnBiO manganites are given in Fig. 7. It is seen that the curves for both manganites are reduced to a single curve. According to the obtained curves for both manganites, it can be said that the magnetic phase transition type is second order. These methods used to determine the magnetic phase transition are consistent with each other.
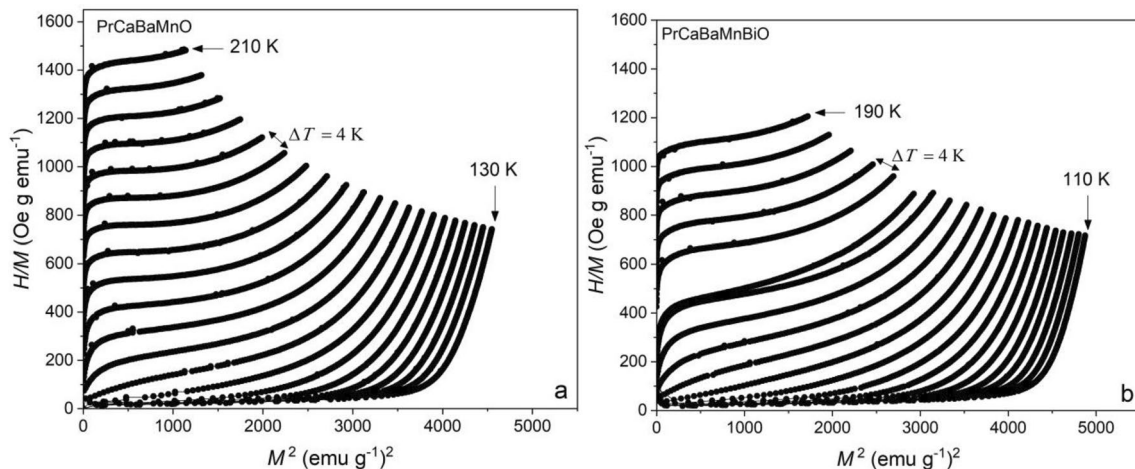

Fig. 6 The Arott plots of PrCaBaMnO (**a**) and PrCaBaMnBiO (**b**) manganites
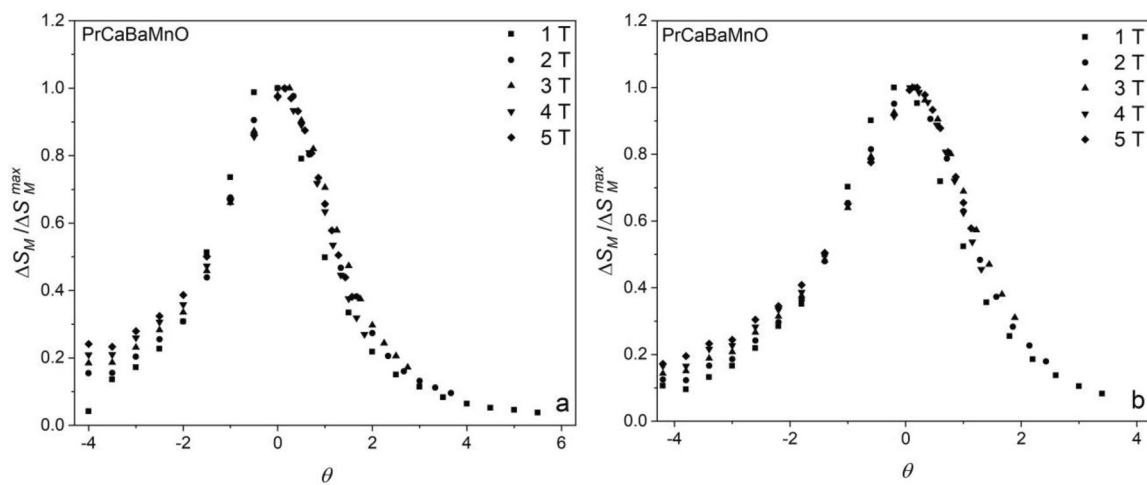

Fig. 7 The $-\Delta S_M(T)/-\Delta S_M^{max}(\theta)$ curves for PrCaBaMnO (**a**) and PrCaBaMnBiO (**b**) manganites

4 Conclusions

In the present work, the structural, magnetic, and magnetocaloric properties of $Pr_{0.55}Ca_{0.05}Ba_{0.40}Mn_{1-x}Bi_xO_3$ (x = 0 and 0.02) manganites prepared by the solid-state reaction method were examined. XRD analyses were performed to determine the crystal structure of manganites and to examine the effect of Bi contribution on lattice parameters and unit cell volume. It is understood from the XRD results that both manganites crystallize in the orthorhombic crystal structure. No change in the crystal structure was induced by Bi doping to the manganese region. However, the unit cell volume of the PrCaBaMnO and PrCaBaMnBiO manganites was decreased with the substitution. In light of the information obtained from SEM analysis, it was observed that a small Bi substitution to the Mn-site caused a decrease in the volume of interparticle spaces and the size of the particles. From $M(T)$ measurements, the T_C values of PrCaBaMnO and PrCaBaMnBiO manganites were identified as 164 and 154 K, respectively. Compared to undoped PrCaBaMnO manganite, a decrease implying deterioration of DE interactions in the T_C value of Bi-doped PrCaBaMnBiO manganite was observed. For the PrCaBaMnO and PrCaBaMnBiO manganites, the $-\Delta S_M^{max}$ values calculated under 2 T magnetic fields were calculated as 3.15 and 2.86 Jkg^{-1}K^{-1}, respectively. The RCP values are 82.4 and 88.6 Jkg^{-1} at 2 T magnetic fields. A higher RCP value was calculated for the PrCaBaMnBiO manganite, implying that the magnetic phase transition occurs in a broader temperature range. According to Banerjee's criterion and Franco's universal master cure, both manganites show SOMT. The $-\Delta S_M^{max}$ and RCP values of the studied manganites are within acceptable limits for low-temperature applications especially (100–200 K).

Author contributions

All authors contributed to conceptualization; SKÇ and GA contributed to experimental design; SKÇ carried out measurements; GA and SKÇ contributed to manuscript composition and material preparation; GA and SKÇ contributed to writing-review and editing; GA, SKÇ, and AE contributed to supervision. All authors have read and agreed to the published version of the manuscript.

Data availability

All data generated or used during the study are available from the corresponding author by request.

Declarations

Conflict of interest   The authors declare that they have no conflict of interest.

Ethical approval   Not Applicable.

References

1. D. Swathi, N.K. Yadav, N. Kumar Swamy, N. Pavan Kumar, *Magnetocaloric Materials For Green Refrigeration* (Elsevier Inc., Amsterdam, 2023)

2. J. Steven Brown, P.A. Domanski, "Review of alternative cooling technologies. Appl. Therm. Eng. **64**, 252–262 (2014)

3. O. Sari, M. Balli, From conventional to magnetic refrigerator technology. Int. J. Refrig. **37**, 8–15 (2014)

4. A. Kitanovski, Energy applications of magnetocaloric materials. Adv. Energy Mater. **10**, 1903741–1903741 (2020)

5. A. Kitanovski, P.W. Egolf, Innovative ideas for future research on magnetocaloric technologies. Int. J. Refrig. **33**, 449–464 (2010). https://doi.org/10.1016/j.ijrefrig.2009.11.005

6. V.I. Zverev, A.P. Pyatakov, A.A. Shtil, A.M. Tishin, Novel applications of magnetic materials and technologies for medicine. J. Magn. Magn. Mater. **459**, 182–186 (2018). https://doi.org/10.1016/j.jmmm.2017.11.032

7. A.M. Tishin, Y.I. Spichkin, *"Magnetocloric Effect and Its Applications"* (IOP publishing, Bristol, 2003), pp.4–401

8. B. Monfared, B. Palm, Material requirements for magnetic refrigeration applications. Int. J. Refrig. **96**, 25–37 (2018). https://doi.org/10.1016/j.ijrefrig.2018.08.012

9. V.K. Pecharsky, K.A. Gschneidner, Advanced magnetocaloric materials: what does the future hold? Int. J. Refrig. **29**(8), 1239–1249 (2006). https://doi.org/10.1016/j.ijrefrig.2006.03.020

10. M.-H. Phan, S.-C. Yu, Review of the magnetocaloric effect in manganite materials. J. Magn. Magn. Mater. **308**, 325–340 (2007). https://doi.org/10.1016/j.jmmm.2006.07.025

11. A.O. Ayaş, S.K. Çetin, G. Akça, M. Akyol, A. Ekicibil, Magnetic refrigeration: current progress in magnetocaloric properties of perovskite manganite materials. Mater. Today Commun. **35**, 105988 (2023). https://doi.org/10.1016/j.mtcomm.2023.105988

12. N. Nedelko, S. Lewinska, A. Pashchenko, I. Radelytskyi, R. Diduszko, E. Zubov, W. Lisowski, J.W. Sobczak, K. Dyakonov, A. Ślawska-Waniewska, V. Dyakonov, H. Szymczak, Magnetic properties and magnetocaloric effect in $La_{0.7}Sr_{0.3-x}Bi_xMnO_3$ manganites. J. Alloys and Compd. **640**, 433–439 (2015). https://doi.org/10.1016/j.jallcom.2015.03.126

13. S. Kılıç Çetin, M. Acet, A. Ekicibil, Effect of Pr-substitution on the structural, magnetic and magnetocaloric properties of (La1-xPrx)0.67Pb0.33MnO3 (0.0 ≤ x ≤ 0.3) manganites. J. Alloys Compd. **727**, 1253–1262 (2017). https://doi.org/10.1016/j.jallcom.2017.08.199

14. G. Akça, Enhancement of magnetic entropy change in $La_{0.5}7Nd_{0.1}Sr_{0.33-x}Ca_xMnO_3$ manganites. J. Mater. Sci. Mater. Electron. **33**, 26495–26512 (2022). https://doi.org/10.1007/s10854-022-09328-w

15. V.E. Salazar-Muñoz, A. Lobo Guerrero, S.A. Palomares-Sánchez, Review of magnetocaloric properties in lanthanum manganites. J. Magn. Magn. Mater. (2022). https://doi.org/10.1016/j.jmmm.2022.169787

16. A. Krichene, P.S. Solanki, S. Rayaprol, V. Ganesan, W. Boujelben, D.G. Kuberkar, B-site bismuth doping effect on structural, magnetic and magnetotransport properties of $La_{0.5}Ca_{0.5}Mn_{1-x}Bi_xO_3$. Ceram. Int. **41**, 2637–2647 (2015). https://doi.org/10.1016/j.ceramint.2014.10.163

17. A. Selmi, R. M'Nassri, W. Cheikhrouhou-Koubaa, N. Chniba Boudjada, A. Cheikhrouhou, Influence of transition metal doping (Fe Co, Ni and Cr) on magnetic and magnetocaloric properties of $Pr_{0.7}Ca_{0.3}MnO_3$ manganites. Ceram. Int. **41**, 10177–10184 (2015). https://doi.org/10.1016/j.ceramint.2015.04.123

18. G. Akça, S.K. Çetin, M. Güneş, A. Ekicibil, Magnetocaloric properties of $(La_{1-x}Pr_x)_{0.85}K_{0.15}MnO_3$ (x=0.0, 0.1, 0.3 and 0.5) perovskite manganites. Ceram. Int. **42**(2016), 19097–19104 (2016). https://doi.org/10.1016/j.ceramint.2016.09.070

19. S.K. Çetin, M. Acet, M. Güneş, A. Ekicibil, M. Farle, Magnetocaloric effect in $(La_{1-x}Sm_x)_{0.67}Pb_{0.33}MnO_3$ (0 ≤ x ≤ 0.3) manganites near room temperature. J. Alloys Compd. **650**, 285–294 (2015). https://doi.org/10.1016/j.jallcom.2015.07.217

20. A.O. Ayaş, A. Kandemir, S.K. Çetin, G. Akça, M. Akyol, A. Ekicibil, Investigation of the effect of sintering temperature on structural, magnetic and magnetocaloric properties in $PrCaMn2O_6$ double perovskite manganite system. J. Mater. Sci. Mater. Electron. **33**, 7357–7370 (2022). https://doi.org/10.1007/s10854-022-07843-4

21. J. Fan, L. Pi, L. Zhang, W. Tong, L. Ling, B. Hong, Y. Shi, W. Zhang, D. Lu, Y. Zhang, Magnetic and magnetocaloric properties in second-order phase transition $La_{1-x}K_xMnO_3$ and their composites. Phys. B Condens. Matter. **532**(2016), 166–171 (2018). https://doi.org/10.1016/j.physb.2017.03.031

22. Y. Fang, M. Li, F. Chen, Observation of Magnetic phase transition and magnetocaloric effect in $Ba_{1-x}Sr_xMnO_{3-\delta}$. J. Supercond. Nov. Magn. **31**, 3787–3792 (2018). https://doi.org/10.1007/s10948-018-4648-1

23. A.I. Abou-Aly, R. Awad, S.A. Mahmoud, M.M. Barakat, EPR studies of (Bi, Pb)-2223 phase substituted by ruthenium ions. J. Alloys Compd. **509**, 7381–7388 (2011). https://doi.org/10.1016/j.jallcom.2011.03.160

24. R.D. Shannon, Revised effective ionic radii in halides and chalcogenides. Acta Cryst. **A32**, 751 (1976)

25. C.H. Shen, C.C. Chen, R.S. Liu, R. Gundakaram, S.F. Hu, J.M. Chen, Internal chemical pressure effect and magnetic properties of $La_{0.6}(Sr_{0.4-x}Bax)MnO_3$. J. Solid State Chem. **156**, 117–121 (2001). https://doi.org/10.1006/jssc.2000.8970

26. A.S. Bhalla, R. Guo, R. Roy, The perovskite structure: a review of its role in ceramic science and technology. Mater.

Res. Innov. **4**, 3–26 (2000). https://doi.org/10.1007/s100190000062

27. S. Tarhouni, A. Mleiki, I. Chaaba, H. Ben Khelifa, W. Cheikhrouhou-Koubaa, M. Koubaa, A. Cheikhrouhou, E.K. Hlil, Structural, magnetic and magnetocaloric properties of Ag-doped $Pr_{0.5}Sr_{0.5-x}Ag_xMnO_3$ manganites (0.0≤x≤0.4). Ceram. Int. **43**, 133–143 (2017). https://doi.org/10.1016/j.ceramint.2016.09.122

28. L.D. Mendonca, A. D'Souza, M.S. Murari, M.D. Daivajna, Magneto transport anomaly of bismuth substituted (La, Na)MnO_3. J. Supercond. Nov. Magn. **33**, 1809–1819 (2020). https://doi.org/10.1007/s10948-020-05430-4

29. A. Degreeeysam, A. Moheb, E. Joudaki, High surface area nano-sized $La_{0.6}Ca_{0.4}MnO_3$ perovskite powder prepared by low temperature pyrolysis of a modified citrate gel. Cent. Eur. J. Chem. **7**, 809–817 (2009). https://doi.org/10.2478/s11532-009-0083-2

30. M.D. Daivajna, V.P.S. Neeraj Kumar, B.G. Awana, J. Benedict Christopher, S.O. Manjunath, K.Z. Syu, Y.K. Kuo, A. Rao, Electrical, magnetic and thermal properties of $Pr_{0.6-x}Bi_xSr_{0.4}MnO_3$ manganites. J. Alloys Compd. **588**, 406–412 (2014). https://doi.org/10.1016/j.jallcom.2013.11.033

31. H. Gencer, S. Atalay, H.I. Adiguzel, V.S. Kolat, Magnetocaloric effect in the $La_{0.62}Bi_{0.05}Ca_{0.33}MnO_3$ compound. Phys. B Condens. Matter. **357**(2005), 326–333 (2005). https://doi.org/10.1016/j.physb.2004.11.084

32. N. Chau, D.T. Hanh, N.D. Tho, N.H. Luong, Spin glass-like behavior, giant magnetocaloric and giant magnetoresistance effect in PrPb manganites. J. Magn. Magn. Mater. **303**, 335–338 (2006). https://doi.org/10.1016/j.jmmm.2006.01.094

33. N.H. Luong, D.T. Hanh, N. Chau, N.D. Tho, T.D. Hiep, Properties of perovskites $La_{1-x}Cd_xMnO_3$. J. Magn. Magn. Mater. **290–291**, 690–693 (2005). https://doi.org/10.1016/j.jmmm.2004.11.338

34. B. Kumar, J.K. Tiwari, H.C. Chauhan, S. Ghosh, Multiple magnetic phase transitions with different universality classes in bilayer $La_{1.4}Sr_{1.6}Mn_2O_7$ manganite. Sci. Rep. **11**, 1–17 (2021). https://doi.org/10.1038/s41598-021-00544-8

35. A. Coşkun, E. Taşarkuyu, A.E. Irmak, S. Aktürk, High magnetic entropy change in $La_{0.70}Ca_{0.21}Ag_{0.09}MnO_3$ compound. J. Alloys Compd. **669**, 217–223 (2016). https://doi.org/10.1016/j.jallcom.2016.01.230

36. S. Kılıç Çetin, G. Akça, M.S. Aslan, A. Ekicibil, Role of nickel doping on magnetocaloric properties of $La_{0.7}Sr_{0.3}Mn_{1-x}Ni_xO_3$ manganites. J. Mater. Sci. Mater. Electron. **32**, 10458–10472 (2021). https://doi.org/10.1007/s10854-021-05702-2

37. J. Fan, L. Xu, X. Zhang, Y. Shi, W. Zhang, Y. Zhu, B. Gao, B. Hong, L. Zhang, W. Tong, L. Pi, Y. Zhang, Effect of A-site average radius and cation disorder on magnetism and electronic properties in manganite $La_{0.6}A_{0.1}Sr_{0.3}MnO_3$ (A = Sm, Dy, Er) (A = Sm, Dy, Er). J Mater Sci **50**, 2130–2137 (2015)

38. I. Kammoun, W. Cheikhrouhou-Koubaa, W. Boujelben, A. Cheikhrouhou, Bi doping effects on the physical properties of $Pr_{0.6}Sr_{0.4}Mn_{1-x}Bi_xO_3$ (0 ≤ x ≤ 0.2) manganese oxides. J. Alloys Compd. **452**, 195–199 (2008). https://doi.org/10.1016/j.jallcom.2006.11.069

39. M.R. Laouyenne, M. Baazaoui, S. Mahjoub, W. Cheikhrouhou-Koubaa, M. Oumezzine, Enhanced magnetocaloric effect with the high tunability of bismuth in $La_{0.8}Na_{0.2}Mn_{1-x}Bi_xO_3$ (0 ≤ x ≤ 0.06) perovskite manganites. J. Alloys Compd. **720**, 212–220 (2017). https://doi.org/10.1016/j.jallcom.2017.05.269

40. F. Saadaoui, M.M. Nofal, R. M'Nassri, M. Koubaa, N. Chniba-Boudjada, A. Cheikhrouhou, Magnetic and magnetocaloric properties of $La_{0.55}Bi_{0.05}Sr_{0.4}CoO_3$ and their implementation in critical behaviour study and spontaneous magnetization estimation. RSC Adv. **9**, 25064–25074 (2019). https://doi.org/10.1039/C9RA04141A

41. A. Bhattacharyya, S. Chatterjee, S. Giri, S. Majumdar, Magnetotransport and magnetocaloric effect in Ho2In. Eur. Phys. J. B **70**, 347–351 (2009)

42. L. Zhang, L. Li, R. Li, J. Fan, L. Ling, W. Tong, Z. Qu, S. Tan, Y. Zhang, Spin–lattice coupling studied by magnetic entropy and EPR in the CdCr 2 S 4 system. Solid State Commun. **150**, 2109–2113 (2010). https://doi.org/10.1016/j.ssc.2010.09.017

43. M.S. Anwar, S. Kumar, F. Ahmed, N. Arshi, G.W. Kim, C.G. Lee, B.H. Koo, "Large magnetic entropy change in $La_{0.55}Ce_{0.2}Ca_{0.25}MnO_3$ Perovskite." J. Magn. **31**, 457–460 (2011). https://doi.org/10.4283/jmag.2011.16.4.457

44. T. Gottschall, K.P. Skokov, M. Fries, A. Taubel, I. Radulov, F. Scheibel, D. Benke, S. Riegg, O. Gutfleisch, Making a cool choice: the materials library of magnetic refrigeration. Adv. Energy Mater. **9**, 1901322 (2019). https://doi.org/10.1002/aenm.201901322

45. B.K. Banerjee, On a generalised approach to first and second order magnetic transitions. Phys. Lett. **12**, 16–17 (1964). https://doi.org/10.1016/0031-9163(64)91158-8

46. V. Franco, J.S. Blázquez, A. Conde, Field dependence of the magnetocaloric effect in materials with a second order phase transition: a master curve for the magnetic entropy change. Appl. Phys. Lett. **89**(22), 222512 (2006). https://doi.org/10.1063/1.2399361

47. C.M. Bonilla, J. Herrero-Albillos, F. Bartolomé, L.M. García, M. Parra-Borderías, V. Franco, Universal behavior

for magnetic entropy change in magnetocaloric materials: an analysis on the nature of phase transitions. Phys. Rev. B **81**(22), 1–7 (2010)

48. H. Yamada, K. Fukamichi, T. Goto, Itinerant-electron metamagnetism and strong pressure dependence of the curie temperature. Phys. Rev. B **65**, 024413 (2001). https://doi.org/10.1103/PhysRevB.65.024413

49. G. Akça, S. Kılıç Çetin, A. Ekicibil, Structural, magnetic and magnetocaloric properties of $(La_{1-x}Sm_x)_{0.85}K_{0.15}MnO_3$ (x = 0.0, 0.1, 0.2 and 0.3) perovskite manganites. Ceram. Int. **43**, 15811–15820 (2017). https://doi.org/10.1016/j.ceramint.2017.08.150

50. V. Franco, A. Conde, J.M. Romero-Enrique, J.S. Blázquez, A universal curve for the magnetocaloric effect: an analysis based on scaling relations. J. Phys. Condens. Matter **20**, 285207 (2008). https://doi.org/10.1088/0953-8984/20/28/285207

51. H. Yang, Q. Wu, N. Yu, Y. Yu, M. Pan, P. Zhang, H. Ge, Study of magnetic and magnetocaloric effect of $Pr_{0.5}Sr_{0.5-x}Na_xMnO_3$ manganites. J. Solid State Chem. **282**, 121072 (2020)

52. R. Thaljaoui, W. Boujelben, M. Pękała, K. Pękała, J. Mucha, A. Cheikhrouhou, Structural, magnetic and transport study of monovalent Na-doped manganite $Pr_{0.55}Na_{0.05}Sr_{0.4}MnO_3$. J. Alloys Compd. **558**, 236–243 (2013). https://doi.org/10.1016/j.jallcom.2013.01.008

53. H. Ben Khlifa, R. M'Nassri, W. Cheikhrouhou-Koubaa, E.K. Hlil, A. Cheikhrouhou, Effects of synthesis route on the structural, magnetic and magnetocaloric properties of $Pr_{0.8}K_{0.2}MnO_3$. Ceram. Int. **43**, 1853–1861 (2017). https://doi.org/10.1016/j.ceramint.2016.10.144

54. R. M'Nassri, W. Cheikhrouhou-Koubaa, M. Koubaa, N. Boudjada, A. Cheikhrouhou, Magnetic and magnetocaloric properties of $Pr_{0.6-x}Eu_xSr_{0.4}MnO_3$ manganese oxides. Solid State Commun. **151**, 1579–1582 (2011). https://doi.org/10.1016/j.ssc.2011.07.027

55. J. Fan, L. Pi, L. Zhang, W. Tong, L. Ling, B. Hong, Y. Shi, W. Zhang, D. Lu, Y. Zhang, Magnetic and magnetocaloric properties of perovskite manganite $Pr_{0.55}Sr_{0.45}MnO_3$. Phys. B **406**, 2289–2292 (2011). https://doi.org/10.1016/j.physb.2011.03.056

56. A. Jerbi, A. Krichene, N. Chniba-Boudjada, W. Boujelben, Magnetic and magnetocaloric study of manganite compounds $Pr_{0.5}A_{0.05}Sr_{0.45}MnO_3$ (A=Na and K) and composite. Phys. B **477**, 75–82 (2015). https://doi.org/10.1016/j.physb.2015.08.022

57. R. M'Nassri, A. Selmi, N.C. Boudjada, a. Cheikhrouhou, Field dependence of magnetocaloric properties of 20% Cr-doped $Pr_{0.7}Ca_{0.3}MnO_3$ perovskite. J. Therm. Anal. Calorim. **129**, 53–64 (2017). https://doi.org/10.1007/s10973-017-6110-1

58. M. Shi, P. Bisht, A. Kumar, R.N. Mahato, Magnetic and magnetocaloric properties of the nanocrystalline $Pr_{0.7}Ba_{0.2}Ca_{0.1}MnO_3$ sample. AIP Adv. **11**, 015239 (2021). https://doi.org/10.1063/9.0000088

59. A. Varvescu, I.G. Deac, Critical magnetic behavior and large magnetocaloric effect in $Pr_{0.67}Ba_{0.33}MnO_3$ perovskite manganite. Phys. B **470–471**, 96–101 (2015). https://doi.org/10.1016/j.physb.2015.04.037

60. R. Jemai, R. M'Nassri, A. Selmi, H. Rahmouni, K. Khirouni, N. ChnibaBoudjada, A. Cheikhrouhou, Composition dependence of physical properties in $Pr_{0.7}Ca_{0.3}Mn_{1-x}Ni_xO_3$. J. Alloys Compd. **693**, 631–641 (2017)